



"HENRI COANDA"
AIR FORCE ACADEMY
ROMANIA



GERMANY



"GENERAL M.R. STEFANIK"
ARMED FORCES ACADEMY
SLOVAK REPUBLIC

INTERNATIONAL CONFERENCE of SCIENTIFIC PAPER
AFASES 2011
Brasov, 26-28 May 2011

METHODS OF INVESTIGATING AT A NANO-LEVEL THE SURFACES OF METALLIC MATERIALS IN LIQUID ENVIRONMENTS

Marius Dan BENȚA*, Camelia GHIOCEL**, Lizica MODEL**

*"Transilvania" University of Brasov, ** Transport Technical College, Brasov

Abstract: The final aim of the research presented in this article is to present some investigation methods of metallic surfaces in liquid environments. It has also taken into consideration preventing unwanted phenomena by first investigating surfaces at a nano – scale through technologies like Atomic Force Microscopy.

Keywords: investigating, metallic materials, Atomic force microscopy.

1. INTRODUCTION

During the scanning process, the scanning area is initially set at step 1 by Xmin, Ymin, Xmax and Ymax values. The scanning is automatically performed by the program row by row. The scanning path is demonstrated in figure 1.

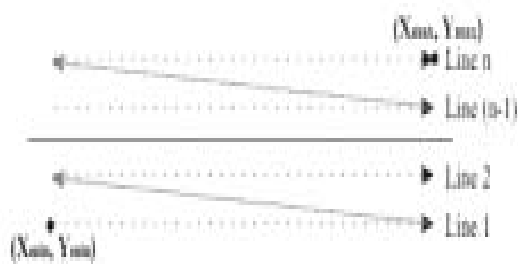


Fig. 1 Scanning Path

If the zooming function, is not chosen the default steps in x and y directions are incremented by 0.0096 V. The following zoom options that are available in the program can be seen in figure 2 (b). The user can select the

value before running the program, but it cannot be changed while the program is running.

The front panel and the block diagram used to set zooming are shown in figure 2.

The maximum resolution (64x zoom) results in steps incremented by $0.0096 \text{ V}/64 = 0.00015 \text{ V}$.

Zoom	
C -4xZoom	1step=37.5 nm Max: 500x250
C -2xZoom	1step=18.75 nm Max: 1000x500
C Default	1step=9.38 nm Max: 2000x1000
<input checked="" type="radio"/> 2xZoom	1step=4.69 nm Max: 4000x2000
C 4xZoom	1step=2.34 nm Max: 8000x4000
C 8xZoom	1step=1.17 nm Max: 16000x8000
C 16xZoom	1step=0.59 nm Max: 32000x16000
C 32xZoom	1step=0.29 nm Max: 64000x32000
C 64xZoom	1step=0.15 nm Max: 128000x64000

(a)

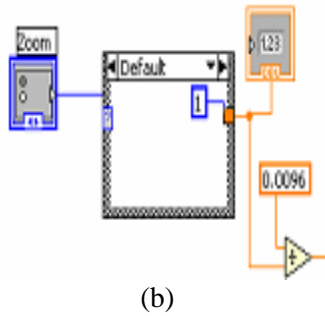


Fig. 2 Zooming Options (a) Front Panel (b) Block Diagram in LabVIEW

The step increment in x and y directions exploits the highest possible resolution with the NI ELVIS system, and it is calculated according to the following formula:

$$\frac{\text{Maximum voltage}}{\text{Resolution} - 1} = \frac{10V}{2^{16} - 1} = 0.000153V \quad (1)$$

Ten volts is the maximum voltage output of the NI ELVIS system. This will be amplified 10 times to the maximum of 100 V by the Physik Instrumente piezo driver device before it is applied to x, y and z expansion of the piezo crystal of the Molecular Imaging scanner head. 0.000153V is the resolution resulting from the 16 bit output of the NI ELVIS system. The scanner head has 2 pairs of piezo actuators, for x and y directions (X+ (pin#8), X-(pin#9) and Y+(pin#4), Y-(pin#5)). However, the piezo amplifier device has only 3 channels. Therefore, two relays are implemented and controlled through a digital output of the NI ELVIS board to share the channels between x- and x+ and also between y- and y+. The voltage function is shown in the following graph.

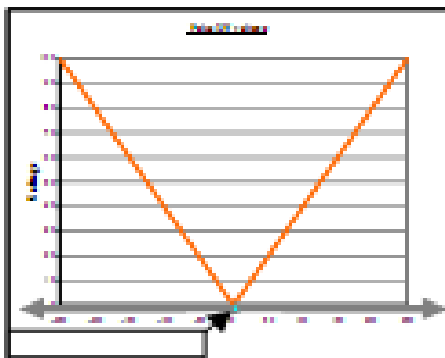


Fig. 3 The voltage function graph

In recent years, scanning probe microscopy (SPM) has become an important tool in materials science. It not only allows ultimate analyses of surface structures to be conducted, but also unique procedures to be performed, such as material deposition, initiation of chemical reactions (e.g. oxidation, lithographic reactions), mechanical structuring as well as manipulation of atoms, molecules, and clusters. Phenomena of practical importance, such as friction, adhesion, local magnetism, and surface diffusion can be studied on a microscopic scale. Several special types of instruments are now available for surface modification and for studying the surface properties of materials. Among other methods of interest in materials science are electrolytic SPM techniques and SPM techniques using magnetic and optical sensors. Descriptions of surface topography were the main objective of earlier studies of scanning probe microscopy. In the past few years, however, more and more quantitative analyses have been performed by means of scanning probe microscopes. In this overview, results will be discussed of nine cases of surface modification and quantitative analysis by scanning tunneling (STM) and scanning force microscopes (SFM, AFM). SPM has a considerable impact now on research and development in micro and nanotechnology. Scanning force microscopes have become important tools for controlling the topography of electronic chips in the production process, and for analysis of the topography of micromechanical components. One of the most promising applications of scanning probe microscopy is in the elucidation of the fundamentals of future nanotechnology. In technology, materials science and solid state physics on an atomic scale should meet. Also studies of chemical and biological nanosystems will contribute to the fundamentals of future nanotechnology. Two aspects are of special interest: Firstly, the self-organization processes occurring in nature and secondly, the creation of nanosystems by surface modification and by manipulation of atoms, molecules or clusters, and the characterization of such artificial systems. It is worthwhile studying biological molecular systems, such as motors, sieves, and electrical



"HENRI COANDA"
AIR FORCE ACADEMY
ROMANIA



GERMANY



"GENERAL M.R. STEFANIK"
ARMED FORCES ACADEMY
SLOVAK REPUBLIC

INTERNATIONAL CONFERENCE of SCIENTIFIC PAPER
AFASES 2011

Brasov, 26-28 May 2011

conductors, to find ways of designing nanosystems for practical use.

A review is presented below the findings made in various subjects of potential interest in nanotechnology, which were studied at our laboratory over the past few years by scanning tunneling and scanning force microscopy.

2. EXAMPLES OF MODIFICATION AND STRUCTURING OF SURFACES

Local Material Deposition and Single Electron Tunneling. Deposition of materials from the tip of the STM was demonstrated nicely; for example, by for the case of Au cluster deposition on polycrystalline Au surfaces. The investigations described in this article are about the generation of small metal clusters on Si (111) surfaces, their thermal stability, and single electron tunneling through them. When the dimension of the metal clusters are on the order of 10 nm or smaller, single electron tunneling effects can be observed even at room temperature. Al- and Au-clusters with diameters between three and several hundred nanometers were generated on Si (111) surfaces by the application of voltage pulses between the tip and the sample. The clusters were stable for more than 24h at room temperature; for small clusters, Coulomb staircase effects were observed in the current versus voltage curves (I(V)). The Al tips, for example, require a bias voltage below -6 V or above +6 V for the deposition process by field evaporation to take place. Figure 4 shows a typical Au cluster as deposited with the STM, and the I(V)-curve together with its derivative demonstrating staircase effects at room temperature.

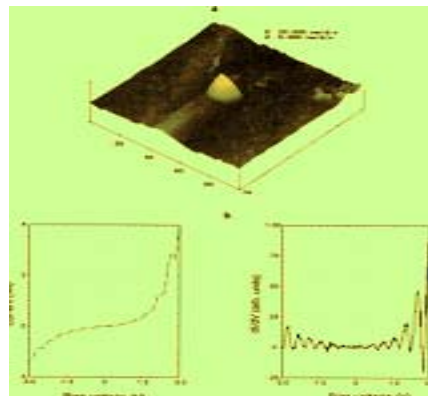


Fig. 4 (a) Au cluster deposited on Si (111) surface by application of a +10 V bias voltage pulse between the Au tip and the substrate (top). (b) I(V) curve measured at room temperature and its derivative showing Coulomb staircase with a step width of 450 mV caused by single-electron tunneling through the cluster

3. MECHANICAL STRUCTURING OF SURFACES

Nanostructures can be generated by ploughing furrows with SFM tips. Also thin Au films deposited on non-conducting substrates were structured to demonstrate the possibility to create conducting nanostructures on an insulating substrate. Figure 5 shows a periodic grid generated on the surface of polycrystalline Au. The profile is quite homogeneous over the area of $2 \mu\text{m} \times 2 \mu\text{m}$. The cantilever tip (Si) shows no pronounced abrasion in the structuring process, as can be concluded from the homogeneity of the structure generated and from the analysis of the tips by scanning electron microscopy. Such periodic grids have been used for measuring the surface self-diffusion constant. Structures generated with the SFM could also be used as molds for making nanostructures out of molecules or clusters as building blocks. Corresponding grid profiles, derived from the images on top (bottom) temperature, however, these procedures are not as sensitive as the

periodic grid method. In these cases, the time dependence of the depth of the profiles, $d(t)$, is given by:

$$d(t) \sim (c_1 t)^{3/4}, \text{ and } d(t) \sim (c_2 t)^{1/4}, \text{ respectively.} \quad (2)$$

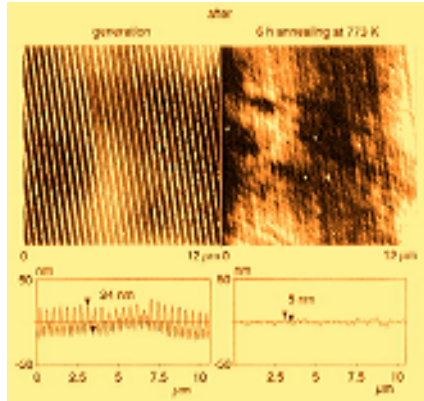


Fig. 5 Mechanical structuring of a polycrystalline Au surface with a stiff SFM cantilever (Si)

Images (top) taken with a soft cantilever (Si₃N₄) of a periodic grid as generated (left), and after annealing (right).

The latter methods are less sensitive because the time dependence is much weaker and no dependence on k exists. Another advantage of studying a periodic grid to determine the diffusion constant is the possibility to derive the grid parameters as a function of temperature by two dimensional Fourier transformations. The results of such analyses represent mean values averaged over the entire area analyzed.

The use of the SFM allows the surface self-diffusion constant to be measured for materials that are soft enough to allow grid generation with a hard cantilever tip, if the surface can be kept clean throughout the measurement so that the diffusion is not altered by contamination.

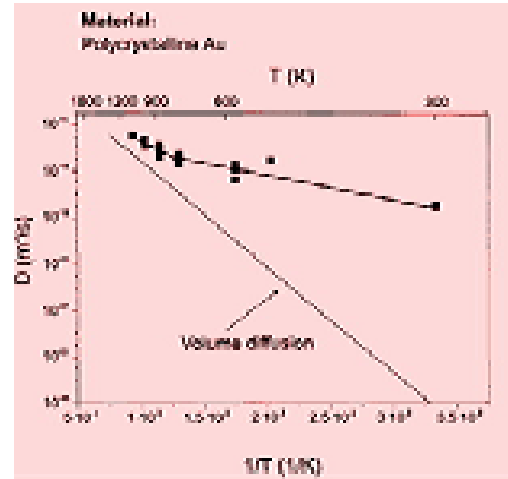


Fig. 6 Self-diffusion constant at the surface of polycrystalline Au as a function of temperature, derived from the decay of the amplitude of the periodic grid shown in figure 5, initiated by vapor deposition of material forming layers or islands

For general application, the measurements would have to be performed in UHV or, at least, in an inert atmosphere. Cluster Dynamics and Ostwald Ripening. Epitaxial growth of islands was studied in great detail on surfaces of single crystals by means of STM. Metal clusters and cluster systems were deposited also on different disordered substrate surfaces, and their structure was analyzed mostly by transmission electron microscopy (TEM). Here we are discussing the dynamics of clusters grown out of ultrathin (10nm thick) Au films deposited on native SiO_x surfaces of Si wafers by annealing the films at relatively low temperatures (50-100° C). The dynamics of these Au cluster systems is determined by the Ostwald ripening process on the substrate surface, characterized, for example, by the growth of the large clusters and the appearance of depletion zones around the growing clusters, as recently observed in SFM experiments. Ostwald ripening is regulated by the vapor pressure, $P(r)$, on surfaces of clusters depending on the curvature of the surface. For spherical clusters with a radius of r , what is given, according to the Gibbs-Thomson equation, by the relation:

$$P(r) = P_{\infty} \exp(2\gamma_s \Omega / r k_B T) \approx P_{\infty} (1 + c/r). \quad (3)$$

A consequence of depending on the radius of the vapor pressure at the cluster surface is



"HENRI COANDA"
AIR FORCE ACADEMY
ROMANIA



GERMANY



"GENERAL M.R. STEFANIK"
ARMED FORCES ACADEMY
SLOVAK REPUBLIC

INTERNATIONAL CONFERENCE of SCIENTIFIC PAPER
AFASES 2011

Brasov, 26-28 May 2011

16 that particles will be transferred from small to large clusters. The large clusters will grow at the expense of the smaller ones which, finally, will dissolve. The largest clusters produced in the generation process have the highest probability of survival during ripening. General theory yields the following time dependence for the growth of the cluster radius, r :

$$r(t) = r_0 t^x \quad (4)$$

The exponent, x , depends on detailed assumptions about the growth process as, for example, discussed in the framework of theories of the ripening process proceeding in two dimensions. In general, two characteristic zones around a growing cluster can be distinguished: a depletion zone defining the area in which material is removed by dissolution of small clusters and a nucleation zone around a growing cluster in what additional clusters may grow, whereas outside nucleation is excluded. If the interaction of the diffusing atoms with the substrate is isotropic, the borderlines between the different zones will be circles whose radii will depend on the diffusion length and the capture probability as a function of the radius of the clusters. Typical results of such ripening process are shown in Figure 7. The borderline around the largest cluster indicating the depletion zone is clearly visible (Figure 7a). Figure 7b shows that at other positions the cluster at the center is surrounded by a ring of clusters indicating the existence of a nucleation zone around the center, outside of which new clusters can not grow. Cluster size distribution, cluster density, cluster growth as a function of annealing time and temperature were studied by SFM analysis.

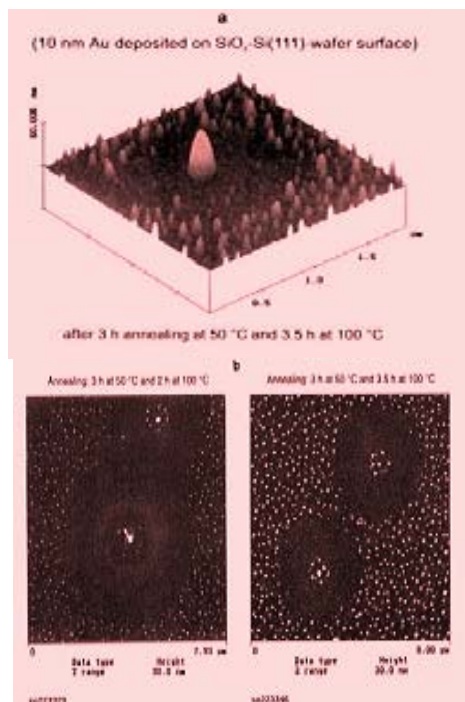
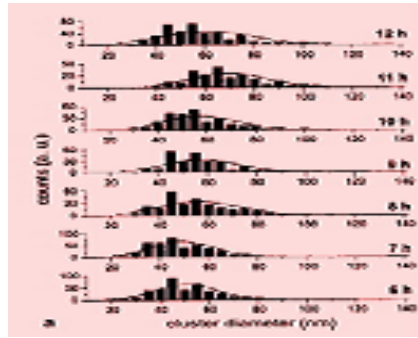
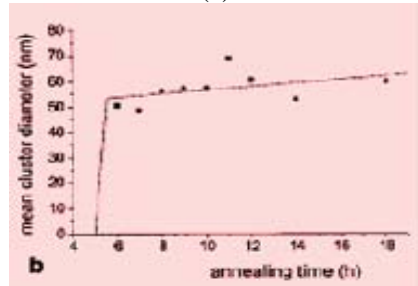


Fig. 7 Ostwald ripening at the surface of an ultrathin Au film from which clusters have been developed. Depletion zones appear around large clusters (a), and, at other positions, also rings of clusters around central clusters have appeared indicating the circular borderline of nucleation exclusion zones (b, left and right)

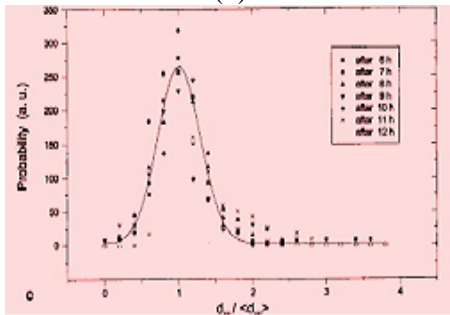
Cluster size and pair distributions as well as the mean cluster diameter as a function of annealing times are shown in Figure 8. The diameter distributions indicate an increase of the number large clusters with increasing annealing time. This change may be a precursor of Ostwald ripening processes. If the ripening processes occur, then the cluster diameter will rise much faster, as observed in another experiment. By characterizing cluster growth dynamics on the substrate surface, one could probably learn how the right kind of metal cluster systems for practical use in catalysis or in single electron tunneling systems could be generated.



(a)



(b)



(c)

Fig. 8 (a) Au cluster diameter distributions for a system in states before the depletion zones appear and (b) mean cluster diameters (derived from a) as a function of the annealing time at an annealing temperature of 50°C. (c). The distribution of inter cluster distances (cluster pair distribution functions) as a function of annealing time indicates the self-similarity of the cluster system in the different states.

4. CONCLUSION

In recent years, scanning probe microscopy (SPM) has become an important tool in materials science. It not only allows ultimate analyses of surface structures to be conducted, but also unique procedures to be performed, such as material deposition, initiation of chemical reactions (e.g. oxidation, lithographic reactions), mechanical structuring as well as manipulation of atoms, molecules, and clusters.

Phenomena of practical importance, such as friction, adhesion, local magnetism, and surface diffusion can be studied on a microscopic scale. Several special types of instruments are now available for surface modification and for studying the surface properties of materials.

Among other methods of interest in materials science are electrolytic SPM techniques and SPM techniques using magnetic and optical sensors.

REFERENCES

1. G. Binnig, C.F. Quate, and Ch. Gerber, Atomic force microscope, *Phys. Rev. Lett.* 56,930-933 (1986);
2. G. Binnig, H. Rohrer, Ch. Gerber, and E. Weibel, Surface studies by scanning tunneling microscopy, *Phys. Rev. Lett.* 49, 57-61 (1982);
3. Helen Hansma, James Vesenka, C. Siegerist, G. Kelderman, H. Morret, R.L. Sinsheimer, V. Elings, C. Bustamante, and P.K. Hansma, Reproducible imaging and dissection of plasmid DNA under liquid with the atomic force microscope, *Science*, 256, 1180-1 184 (1992);
4. E. Henderson, Imaging and nanodissection of individual supercoiled plasmids by atomic force microscopy, *Nuc. Acids Res.* 20,445-447 (1 992);
5. Y.L. Lyubchenko, B.L. Jacobs, and S.M. Lindsay, Atomic force microscopy of reovirus dsRNA: A routine technique for length measurements, *Nucleic Acids Res.*, 20, 3983-3986 (1992);
6. T. Thundat, D.P. Allison, R.J. Warmack, and T.L. Ferrell, Imaging isolated strands of DNA molecules by atomic force microscopy, *Ultramicroscopy*, 42-44, 1101-1 106 (1992);
7. J. Vesenka, M. Guthold, C.L. Tang, D. Keller, E. Delaine, and C. Bustamante, Substrate preparation for reliable imaging of DNA molecules with the scanning force microscope, *Ultramicroscopy*, 42-44, 1243-1249 (1992);
8. J. Yang and Z. Shao, Effect of probe force on the resolution of atomic force



"HENRI COANDA"
AIR FORCE ACADEMY
ROMANIA



GERMANY



"GENERAL M.R. STEFANIK"
ARMED FORCES ACADEMY
SLOVAK REPUBLIC

INTERNATIONAL CONFERENCE of SCIENTIFIC PAPER
AFASES 2011

Brasov, 26-28 May 2011

- microscopy of DNA, Ultramicroscopy, 50. 157-170 (1993);
9. F. Zenhausern, M. Adrian, Heggeler-Bordier, R. Emch, M. Jobin, M. Taborelli, and P. Descouts, Imaging of DNA by scanning force microscopy, J. Structural Biology, 108, 69-73 (1992);
 10. D.P. Allison, L.A. Bottomley, T. Thundat, G.M. Brown, R.P. Woychik, J.J. Schrick, K.B. Jacobson, and R.J. Warmack, Immobilization of DNA for scanning probe microscopy, Proc. Natl. Acad. Sci. U.S.A., 89, 10129-10133 (1992);
 11. T.W. Jing, A.M. Jeffrey, J.A. DeRose, Y.L. Lyubchenko, L.S. Shlyakhtenko, R.E. Harrington, E. Appella, J. Larsen, A. Vaught, D. Rekes, F.-X. Lu, and S.M. Lindsay, Structure of hydrated oligonucleotides studies by in situ scanning tunneling microscopy, Proc. Natl. Acad. Sci. U.S.A., 90.